Journal of Power Sources 273 (2015) 697–706

Contents lists available at ScienceDirect

Journal of Power Sources

journal homepage: www.elsevier.com/locate/jpowsour

Bacterial nanocellulose/Nafion composite membranes for low temperature polymer electrolyte fuel cells

Gao-peng Jiang [a, b, c], Jing Zhang [b], Jin-li Qiao [b, **], Yong-ming Jiang [a], Hadis Zarrin [c], Zhongwei Chen [c], Feng Hong [a, d, *]

[a] Group of Microbiological Engineering and Industrial Biotechnology, College of Chemistry Chemical Engineering and Biotechnology, Donghua University, North Ren Min Road 2999, Shanghai 201620, China
[b] College of Environmental Science and Engineering, Donghua University, North Ren Min Road 2999, Shanghai 201620, China
[c] Department of Chemical Engineering, University of Waterloo, 200 University Avenue West, Waterloo, ON N2L 3G1, Canada
[d] State Key Laboratory for Modification of Chemical Fibers and Polymer Materials, Donghua University, Shanghai 201620, China

HIGHLIGHTS

- A series of novel nanocomposite membranes of BC and Nafion are fabricated for DMFC.
- The novel BC/Nafion membranes were reinforced with concrete-like structure.
- Membranes show high strength, good proton conductivity and low methanol permeability.
- The annealed membranes are more suitable for DMFC.
- High PEMFC and DMFC performances are obtained from annealed B1N7 membranes.

ARTICLE INFO

Article history:
Received 27 May 2014
Received in revised form
5 September 2014
Accepted 22 September 2014
Available online 30 September 2014

Keywords:
Bacterial cellulose
Nafion
Blend membrane
Proton conductivity
Annealing
Membrane electrode assembly

ABSTRACT

Novel nanocomposite membranes aimed for both proton-exchange membrane fuel cell (PEMFC) and direct methanol fuel cell (DMFC) are presented in this work. The membranes are based on blending bacterial nanocellulose pulp and Nafion (abbreviated as B*x*N*y*, where *x* and *y* indicates the mass ratio of bacterial cellulose to Nafion). The structure and properties of B*x*N*y* membranes are characterized by FTIR, SEM, TG, DMA and EIS, along with water uptake, swelling behavior and methanol permeability tests. It is found that the B*x*N*y* composite membranes with reinforced concrete-like structure show excellent mechanical and thermal stability regardless of annealing. The water uptake plus area and volume swelling ratios are all decreased compared to Nafion membranes. The proton conductivities of pristine and annealed B1N9 are 0.071 and 0.056 S cm^{-1}, respectively, at 30 °C and 100% humidity. Specifically, annealed B1N1 exhibited the lowest methanol permeability of 7.21 × 10^{-7} cm^2 s^{-1}. Through the selectivity analysis, pristine and annealed B1N7 are selected to assemble the MEAs. The performances of annealed B1N7 in PEMFC and DMFC show the maximum power densities of 106 and 3.2 mW cm^{-2}, respectively, which are much higher than those of pristine B1N7 at 25 °C. The performances of the pristine and annealed B1N7 reach a level as high as 21.1 and 20.4 mW cm^{-2} at 80 °C in DMFC, respectively.

1. Introduction

Proton conducting membrane is one of the essential and critical materials in both proton exchange membrane fuel cell (PEMFC) and direct methanol fuel cell (DMFC). Compared to PEMFC, DMFC is considerably more suitable for powering portable electric devices, such as laptops and cameras, because of its high power density [1,2]. However, the methanol crossover caused by the intrinsic property of commercial membranes, i.e. Nafion, results in about

* Corresponding author. Group of Microbiological Engineering and Industrial Biotechnology, College of Chemistry Chemical Engineering and Biotechnology, Donghua University, North Ren Min Road 2999, Shanghai 201620, China. Tel./fax: +86 21 67792649.
** Corresponding author. Tel.: +86 21 67792379; fax: +86 21 67792159.
E-mail addresses: qiaojl@dhu.edu.cn (J.-l. Qiao), fhong@dhu.edu.cn, 13564564971@139.com (F. Hong).

http://dx.doi.org/10.1016/j.jpowsour.2014.09.145
0378-7753/

40% loss of fuel when 2 M methanol aqueous solution is fed. The migrated methanol poisons the cathode catalyst by being oxidized inducing an overpotential at the electrode [2,3]. Moreover, in the presence of ruthenium (Ru) in the anode catalyst, which is advantageous to reduce carbon monoxide (CO) poisoning, Ru can be carried by methanol crossover and thus the DMFC performance significantly diminishes [2]. Additionally, high cost of Nafion, \$600–1200 m^{-2}, is another barrier for its extended applications [2]. Therefore, novel proton exchange membranes (PEMs) with high ion conductivity and low methanol permeability are vitally required to be developed.

To date, different methodologies and strategies have been applied to fabricate PEMs for DMFC, either via grafting [4], cross-linking [5], or combining polymer electrolytes with nanoparticles [6], carbon nanotube [7], graphene oxide [8], and acid–base complex [9], or by employing layer-by-layer (LBL) [10], and blending [11] methods. Among them, blending is an easy and efficient technique to improve PEMs properties. One strategy is to blend Nafion with methanol blocking materials such as PVA [12,13], PTFE [14], PVDF [15] and SiO_2 [6], and the other one is to blend proton donors with hydrocarbon polymers including PVA [5,16,17], PBI [18] and SPEEK [19].

Bacterial cellulose (BC), mainly generated by the genus *Gluconacetobacter*, (formerly *Acetobacter* sp.), in particular *G. xylinus* and *G. hansenii*. Furthermore, it could be produced from a traditional beverage culture called Kombucha that is a symbiont of *Gluconacetobacter* and one or more yeasts [20]. Essentially, BC is a kind of pure cellulose material with special 3D nanostructure morphology formed by nanofibrils with the diameter of 20–100 nm [21–23]. Its distinguished properties from plant cellulose include high crystallinity, high tensile strength, high water binding capacity, low gas permeation and good biocompatibility [23]. BC has been reported to be used as a pervaporation membrane to separate ethanol and water [24,25], which implies that BC membrane is capable to have a low alcohol permeability. In addition, a sulfonated regenerated cellulose membrane and a cellulose acetate membrane that have a similar structure as BC, have been reported to work as a potential membrane and a separator in DMFC respectively [26,27]. Combining those two examples, it is reasonable to deduce the possible application of BC in DMFC. Most recently, 2-acrylamido-2-methyl-1- propanesulfonic acid-grafted BC membranes was synthesized and reported its application in DMFC, which partially testified the deduction above [29]. To prove the potential application of BC in DMFC, an easy and direct fabrication methodology needs to be developed.

In this work, a series of BC/Nafion nanocomposite membranes have been prepared by incorporating BC pulp into Nafion solution, and their potentials both in PEMFC and DMFC were evaluated. Since the annealing process has significant effects on Nafion contained membranes [29], the differences between pristine and annealed BC/Nafion membranes were studied and characterized thoroughly by FTIR, TGA, DMA, SEM, water uptake capability, swelling property, proton conductivity, methanol permeability and selectivity, as well as single cell tests in PEMFC and DMFC systems.

2. Experimental

2.1. Fermentation and purification of bacterial cellulose

Kombucha was purchased from local market and used to produce large amounts of bacterial cellulose pellicles in this study. The fermentation medium was the same as the seed medium and the preparation was as follows. Cool tea infusion was made by soaking 0.5% (w/v) green tea in boiling deionized (DI) water for 20 min and then was used to dissolve 5% (w/v) D-glucose, 0.5% (w/v) yeast extract (Oxoid, UK), and 0.3% (w/v) tryptone (Oxoid, UK). Then the brownish liquid culture medium was split into pre-autoclaved flasks with lids followed by pasteurization without pH regulation.

A Kombucha pellicle preserved in a seed medium was chosen as the seed inoculum. The pellicle was cut into small pieces with a sterilized scissor in a sterile hood and one or two pieces were inoculated into a 100 mL fermentation medium. After static incubation at 30 °C for seven to ten days, thick yellowish BC pellicles formed at the top of the cultures.

BC pellicles were harvested and rinsed with the DI water to remove soluble medium components and then treated in 1.0% sodium hydroxide solution for 2 h at 80 °C to eliminate attached bacterial cells and other impurities. Thereafter, BC pellicles were further purified by boiling in the DI water for 2 h. The purification process was repeated until the BC samples changed to milky color or semitransparent. Finally, the BC hydrogels were rinsed with the DI water until the pH value of the eluent was neutral and the absorbance at 280 nm of the eluent was the same as water. The purified BC pellicles were stored in the DI water at 4 °C for further use.

2.2. Preparation of bacterial cellulose pulp

Similar to the method used by Helbert et al. [30], a food blender was applied to homogenize BC. Small pieces of BC pellicles and DI water of threefold weight of the BC gel were placed into the food blender, and then the BC pulp was prepared by continuously cutting at a full speed for 30 min until no big gel piece was observed. The homogenous BC pulp was poured into a sterilized container with a lid, sealed with parafilm and preserved at 4 °C. Triplicate pulp samples of 10 mL were dried at 105 °C overnight and weighed to determine the content of dry mass in the BC pulp. An appropriate BC concentration range was 3–5 mg L^{-1}.

2.3. Preparation of BC/Nafion blending membranes

Considering the insolubility of Nafion in water, different amounts of 5% Nafion solution (Dupont) were added in the mixture of BC pulp, n-propanol and ethanol (45:48:2, w/w) and stirred at low speed under room temperature overnight. The homogenous suspension was concentrated by vacuum distillation in a rotary evaporator at 50 °C followed by cooling and degasing in a vacuum drying oven for 15 min. Then, the condensed pulp was transferred into glass Petri dishes and de-bubbled with capillary tubes in order to cast into the BC/Nafion blend membranes under room temperature.

Few days later, the formed BC/Nafion membranes were peeled off from the petri dishes carefully after immersing in DI water overnight. In order to eliminate soluble impurities, the harvested BC/Nafion membranes were rinsed with DI water until no alcohol could be detected in the immersion liquid by comparing O.D. value of rinsing water with that of the blank control group at 525 nm after they were reacted with acidic potassium permanganate. Thereafter, the BC/Nafion membranes were dried at ambient temperature and half of them were annealed at 110 °C for 1 h just like the PVA/Nafion blends [29].

2.4. Characterization of BC/Nafion membranes

The BC/Nafion membranes were characterized by attenuated total reflection fourier transform infrared (ATR-FTIR) spectra. The membrane samples were placed on an infrared spectrometer (NEXUS-670, Nicolet-Thermo) covering the diamond of ATR instrument, then spectrograms with a wavenumber resolution of 4 cm^{-1} in the range from 4000 to 650 cm^{-1} were obtained.

A thermogravimetric analysis (TGA) of membranes was carried out on an analyzer (TG 209, NETZSCH). Sample of 5 mg was loaded into an alumina oxide pan and then was heated from 25 to 700 °C at a heating rate of 10 °C min^{-1} under a protection of nitrogen flow at 20 mL min^{-1} [31].

Membrane samples for dynamic thermal mechanical analysis (DMA) were cut into strips with 2–3 cm long and 2–8 mm wide and dried under vacuum at 60 °C overnight. BC/Nafion membranes were loaded on a DMA apparatus (Q800, TA) and tested with a stable frequency of 1 Hz, a preloaded force of 0.01 N, a detectable stress of 0.01 N, a heating rate of 2 °C per minute and temperature range from −50 °C to 150 °C in a model of multi frequencies-stress.

Cross-sectional images of the membranes were inspected by using FEI Quanta 250 scanning electron microscope (SEM), which was operated at 10 kV under high vacuum circumstance. The specimens were sputtered with gold followed by observing at low (×1000 or 2000) and high (×10000) magnifications.

2.5. Water uptake and dimensional stability

Both the BC/Nafion membranes before and after annealing were soaked in DI water for at least 24 h. They were picked out to measure the thickness and then transferred to a smooth glass plate to measure the length and width. The water on the surface was carefully removed with filter paper and the membranes were immediately weighed. After drying samples at 60 °C overnight, the length, width, thickness and weight of the membranes were measured. Then, the water uptake (WU) of membranes (g g^{-1}) was calculated as follows:

$$\mathrm{WU} = \left(W_{\mathrm{wet}} - W_{\mathrm{dry}}\right) \Big/ W_{\mathrm{dry}} \tag{1}$$

where W_{wet} and W_{dry} represent the masses of the swollen and dried membranes, respectively [34]. The area swelling ratio (ASR) and volume swelling ratio (VSR) were calculated according to the following equations:

$$\mathrm{ASR} = \frac{A_{\mathrm{wet}} - A_{\mathrm{dry}}}{A_{\mathrm{dry}}} \times 100\% \tag{2}$$

$$\mathrm{VSR} = \frac{V_{\mathrm{wet}} - V_{\mathrm{dry}}}{V_{\mathrm{dry}}} \times 100\%, \tag{3}$$

where A_{wet}, V_{wet} and A_{dry}, V_{dry} are the area and volume of the fully hydrated membranes and the dry membranes, respectively [33].

2.6. Proton conductivity

The proton conductivity of BC/Nafion membranes was measured by using an electrochemical impedance analyzer (PAR2273, Prinston) under test conditions that AC frequency was scanned from 100 kHz to 0.1 Hz at voltage amplitude of 100 mV. Both the BC/Nafion membranes before and after annealing were cut into pieces with a size of 1 × 1.5 cm and were sandwiched in a Teflon conductivity cell equipped with Pt foil contacts where Pt black was plated [17,31]. The proton conductivity (S cm^{-1}) was calculated using the following expression:

$$\sigma = l/Rbd \tag{4}$$

where l is the distance between two potential sensing platinum foils, R is the membrane resistance, b and d are the width and the thickness of the membrane, respectively [31].

2.7. Methanol permeability and selectivity

Methanol permeability of BC/Nafion membranes was measured by using a home-made liquid diffusion cell which consisted of two mirror symmetric glass compartments with a capacity of approximate 300 mL for each one. The membranes, equilibrated in DI water for at least 24 h prior to the test, were attached on the ground glass surfaces of two compartments, and sandwiched between the compartments vertically by sealing with O-rings. The two compartments were connected and immobilized with flanges, which left an effective area of 8.74 cm^2 to work [32]. The left compartment was fed with aqueous methanol solution (1 mol L^{-1}) while the right one was filled with pure DI water, which were both well-stirred during the test. With methanol diffusion from the left to the right driven by the concentration difference, the methanol concentration in the right compartment increased gradually and appeared a linear relationship with time. Combining with timing sampling and determination of the concentration of permeating methanol with gas chromatography (7890A, Agilent Technologies), a plot of methanol concentration in the right compartment as function of time could be depicted and the methanol permeability (P_M/ cm^2 s^{-1}) could be calculated with slope (S) of the plot by the following equation:

$$P_M = S\frac{V_R d}{AC_L} \tag{5}$$

where A and d are the membrane area and thickness, respectively, while c_L and V_R represent the initial concentration of methanol in the left compartment and the volume of DI water in the right compartment respectively [34].

The selectivity (α) was a measurable standard of membranes to evaluate their potential application in DMFC, which was defined as the ratio of proton conductivity (σ) to methanol permeability (P_M) [35,36], shown as follows.

$$\alpha = \sigma / P_M \tag{6}$$

2.8. MEA fabrication and single-cell performance tests for PEMFC and DMFC

The fabrication of MEAs was as follows. The anode catalyst layer deposited on the carbon paper (Toray TGP-H-090) was the mixture of 30%Pt/15%Ru/C catalyst (Johnson Matthey) and Nafion (DuPont) with the ratio of 3:1 and metal loading of 1.72 mg cm^{-2} while the cathode catalyst layer was the mixture of 40%Pt/C catalyst (Johnson Matthey) and Nafion with Pt loading of 0.95 mg cm^{-2} instead. The BC/Nafion membranes before or after annealing with a size of 4 × 4 cm were sandwiched with those carbon papers coated with catalyst and binder prior to being hot-pressed at a pressure of 10 MPa at 100 °C for 3 min [37].

The MEAs with an active area of 4 cm^2 were activated and evaluated in a single H_2/O_2 fuel cell where the performance of PEMFC was observed under the test condition that pure hydrogen and oxygen were supplied to enter the anode and cathode channels at a flux of 100 and 70 mL min^{-1}, respectively, through a humidifier worked at 25 °C under ambient pressure. Thereafter, the fuel was changed from hydrogen to aqueous methanol solution (1 mol L^{-1}) at the flux of 5 mL min^{-1} and the flux of oxygen increased to 100 mL min^{-1} to test the DMFC performance of BC/Nafion membranes at ambient temperature, 60 °C and 80 °C, respectively. All the polarization curves and power density curves were obtained using a fuel cell evaluation system (GE/FC1-100) [31,36].

3. Results and discussion

3.1. ATR-FTIR

Typical ATR-FTIR spectra of different BC/Nafion membranes before and after annealing, Nafion 115, and casted BC membrane are displayed in Fig. 1. The characteristic bands of cellulose at 3345, 2847–2921, 1162, 1110, 1059, 1035 cm^{-1} were observed in the casted BC membrane, where were assigned as ν_s(O–H), ν_s(C–H) in methylene and methylidyne, ν_{as} (C–O–C) at β-glycosidic linkage, ν_s (C–C) of glucose ring, ν_s(C–O) of secondary alcohol at C-2, C-3 and primary alcohol at C-6, respectively [31,38–40]. Besides, other marked peaks in fingerprint region such as in-plane bending vibration of CH_2 at 1483 and 1425 cm^{-1} and wagging vibration of CH_2 at 1316 cm^{-1} as well as the water molecular absorbance at 1638 cm^{-1} were found in the casted BC membrane. As to Nafion 115 membrane, a board peak around 3454 cm^{-1} assigned as the stretching vibration of hydroxyl in sulfoacid groups and the absorbed water molecules was observed. Several other characteristic bands of Nafion were found too. According to the reference, the bands at 1213, 1153, 1058 cm^{-1} meant the existence of sulfoacid groups in the membrane, which represented the asymmetric stretching vibration, the symmetric stretching vibration of S=O in sulfoacid groups after absorbing with water and the stretching vibration of S–O, respectively [41]. Meanwhile, as mentioned in references, peaks at 1213, 1153 cm^{-1} might be attributed to the asymmetric and symmetric stretching vibration of C–F on the skeleton of PTFE in Nafion too. The sharp shoulder peaks at 983 and 971 cm^{-1} were the typical absorbance of C–O–C on the side chain of Nafion [41–43]. Some peaks of BC and Nafion were overlapped: 3300–3400 cm^{-1}, 1150–1160 cm^{-1}, 1055–1060 cm^{-1}. Therefore, peaks around 2800–3000, 1110 and 1034 cm^{-1} could be used to prove the existence of BC while bonds around 1213, 983 and 971 cm^{-1} could illustrate the existence of Nafion.

As shown in Fig. 1, both membranes B1N1 and B1N7 displayed the characteristic peaks of BC and Nafion regardless of being annealed or not. This result clearly demonstrates the existence of both substances in the blend membranes. Compared to B1N7, B1N1 membranes with lower proportion of Nafion, the characteristic bands of both BC and Nafion were intense and marked, even those peaks ranging from 1300 to 1500 cm^{-1}, whose spectra resembled the one of BC. However, by increasing the Nafion loading, the intensity of some characteristic bands of BC have been either lessened or shadowed by Nafion peaks, such that ν(O–H), ν(C–H) and ν_s(C–O) of primary alcohol were remained to verify the existence of BC. In the prepared BC/Nafion blend membranes, some characteristic peaks still existed, such as ν_s (C–C) of glucose ring of BC at 1110 cm^{-1} and ν (C–O–C) of side chain of Nafion at 983 cm^{-1} whilst some other bands were shifted. For instance, the symmetric stretching vibration of hydroxyl was red-shifted from 3345 cm^{-1} in BC and 3454 cm^{-1} in Nafion to 3339 cm^{-1} in B1N1 and 3343 cm^{-1} in B1N7, respectively. Likewise, the asymmetric stretching vibration of C–F and S=O at 1213 cm^{-1} was shifted to 1224 cm^{-1} in B1N1 and 1217 cm^{-1} in B1N7 respectively, i.e. the blue-shift effect. Those red and blue shifts perfectly proved the hydrogen bonds between the C–F or sulfoacid groups of Nafion and the hydroxyls of BC.

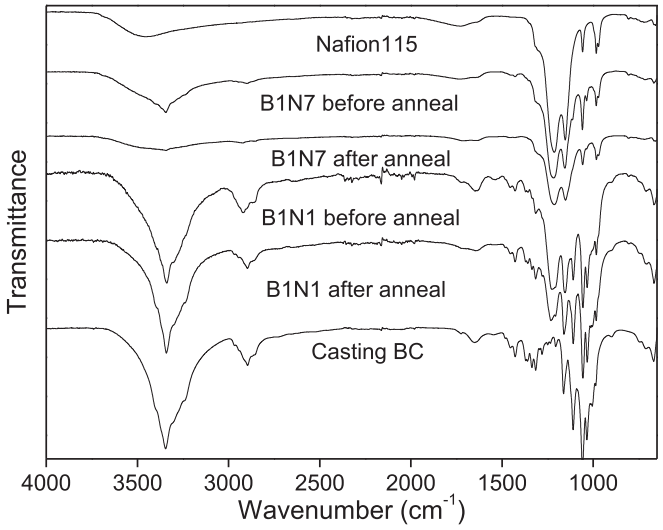

Fig. 1. ATR-FTIR spectra of casted BC, Nafion 115 and different BC/Nafion membranes before and after annealing. B1N1 and B1N7 represent BC/Nafion membranes with a ratio of BC to Nafion of 1:1 and 1:7, respectively.

Moreover, Fig. 1 indicates, no remarkable changes in the spectrum of B1N1 after annealing were observed compared to that before annealing, except for slightly lower intensity of some peaks. However, samples with high ratio of Nafion, i.e. B1N7, showed distinguished changes in the spectra after annealing. Most of the characteristic peaks of BC in the annealed membrane were shadowed or vanished which left merely the weak absorption bands of hydroxyl and methylene as the proof of the existence of BC. Furthermore, the intensity of bands assigned as ν_s(O–H), ν_{as} (C–F) or ν_{as} (S=O) was much lower than that of the pristine one, which indicates the heating process might trigger some reaction between hydroxyls and sulfoacid groups like esterification or dehydration reaction [44]. The low intensity might be ascribed to the low proportion of BC (approximately one eighth) too. According to literature, the side and main chains of Nafion start to gradually degrade after been heated up to 320 °C and higher temperatures, respectively [42,44]. However, in this study the peak intensity at 983 cm^{-1} did not significantly shift or reduce, indicating that the annealing process did not drastically affect the side chain or the main skeleton of Nafion.

3.2. Thermal stability

The thermal stabilities of the BC/Nafion blend membranes were investigated before and after annealing by using thermogravimetric analysis and the results are displayed in Fig. 2. As shown in Fig. 2, there was only one significant weight loss stage in both TG and DTG curves of casted BC, beginning at 280 °C and ending at 400 °C, which is in agreement with references [31,45]. For Nafion 115, three typical weight loss stages were observed, including water evaporation below 120 °C, degradation of side chain from 280 to 380 °C and decomposition of the PTFE skeleton ranging from 380 to 560 °C, which were consistent with TGA-IR results reported by Perusich [41]. Therefore, the two raw materials were thermally stable below 250 °C.

However, the situation changed after blending. Not only the typical weight loss stages of BC and Nafion occurred at lower temperature, but also a new weight loss stage emerged between 120 and 200 °C. The more proportion of Nafion in the blend membranes, the lower temperature the new weight loss stage started, which could be clearly distinguished by the DTG curves of B1N1 and B1N5 in Fig. 2b. This might result from the dehydration reaction between sulfoacid groups of Nafion and the hydroxyls of BC, or acid catalysis of Nafion just like inorganic acid to the degradation of cellulose [31,44]. In addition, the DTG profile of B1N5 displayed three typical pyrolysis peaks while that of B1N1 appeared multi-peaks, which needs to be analyzed by using TGA-IR or other tests in a further study. However, no matter how much weight of B1N1 was lost, they were still thermally stable under the normal operating temperature of DMFC (<100 °C).

The effect of annealing on BC/Nafion blend membranes could be observed from TG and DTG curves. As shown in Fig. 2, after

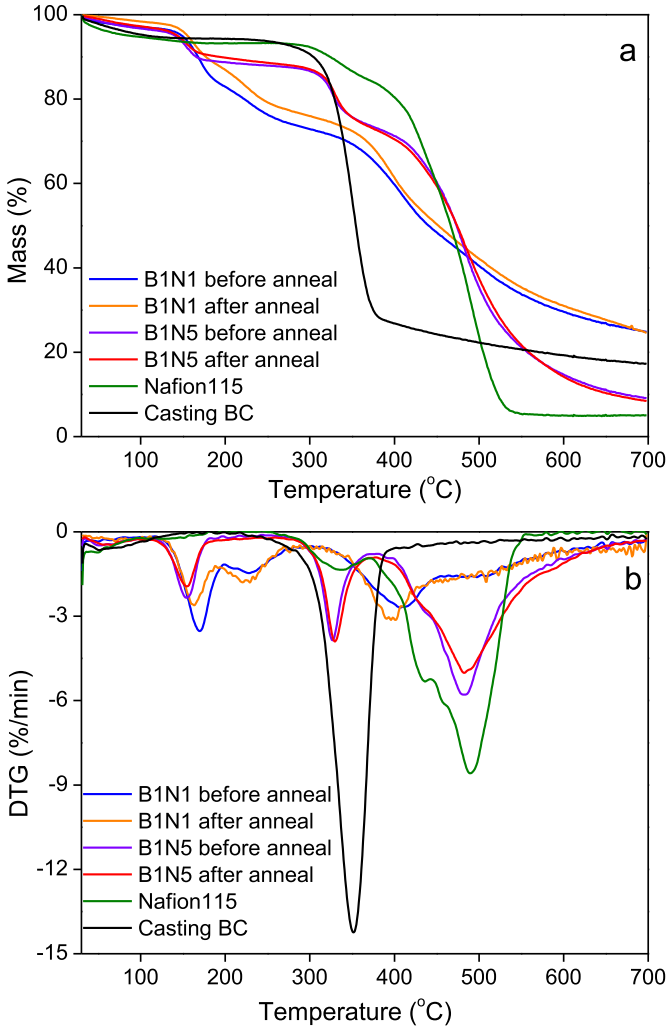

Fig. 2. TGA profiles of casted BC, Nafion 115 and different BC/Nafion membranes before and after annealing. B1N1 and B1N5 represent BC/Nafion membranes with a ratio of BC to Nafion of 1:1 and 1:5, respectively.

annealing, the blend membranes with different ratio of BC to Nafion displayed different characteristic weight loss stages and DTG peaks. However, they were quite similar to the ones before and after annealing, and the annealed B1N5 even coincided with the pristine one. In the DTG curves, the shift of weight loss peaks to lower temperature was found in the annealed B1N1 samples as compared to the samples before annealing. For instance, the temperature at maximum weight-loss rate (T_{max}) for three main peaks decreased from 170, 228 and 406 °C to 163, 221 and 396 °C, respectively. Whereas, the T_{max} of B1N5 did not change remarkably after annealing, indicating that the heating process had less influence on the BC/Nafion blend membranes with high ratio of Nafion. It is noteworthy that the amounts of weight loss of most peaks were marginally lessened after annealing, especially the new weight loss peaks in both B1N1 and B1N5. This implies that the annealing process might be helpful to eliminate the new weight loss stage. Hence, the stability of annealed BC/Nafion membranes was qualified for the application in DMFC.

3.3. Dynamic mechanical thermal analysis

The DMA profiles of Nafion 115, casted BC, pristine and annealed B1N1 membranes are displayed in Fig. 3, including storage modulus and loss factor as function of temperature. Normally, DMA test is a best choice for the investigation of glass transition of polymers with high degrees of crystallinity or cross-linking, because the change of loss factor near glass transition point is much more sensitive than enthalpimetric analysis like DSC [46]. Given the stretching test model, the storage moduli of membranes could represent their Young's moduli. Hence, the DMA test could give the information of both glass transition and mechanical properties of membranes.

As shown in Fig. 3a, the storage modulus of Nafion 115 was about 220 MPa under the ambient temperature and declined slowly as temperature increased, but dropped sharply at a higher

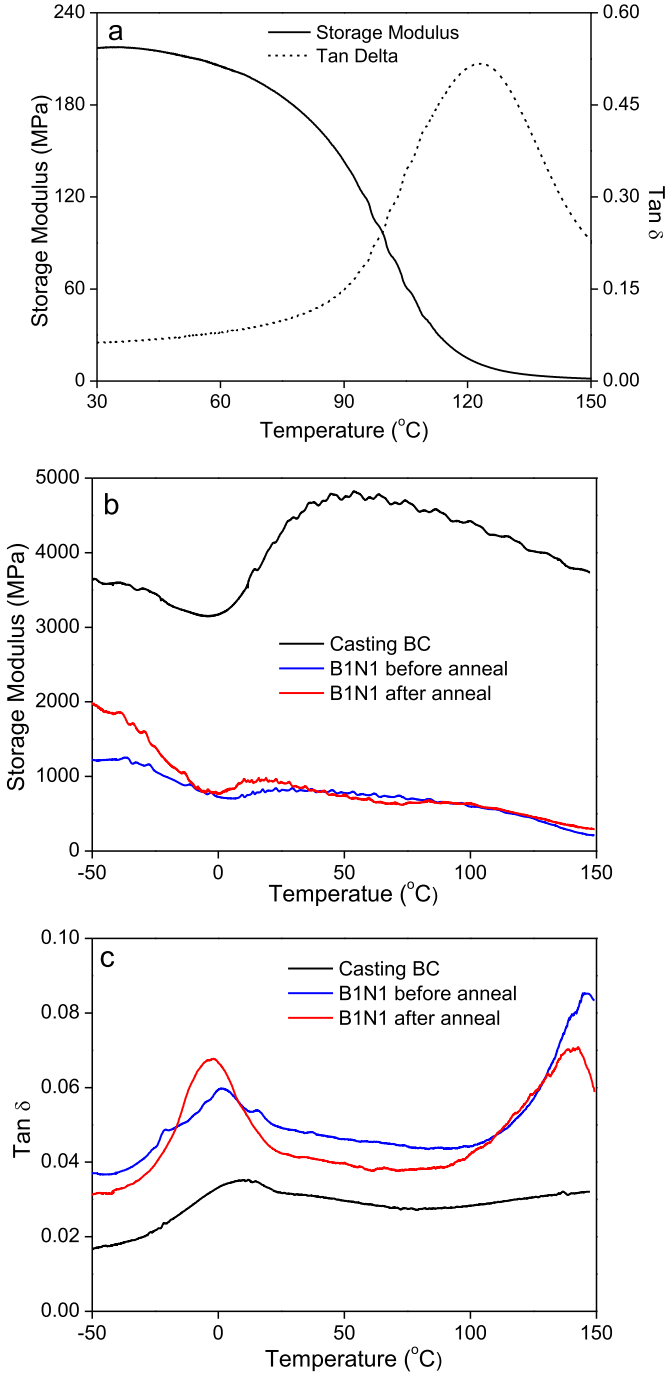

Fig. 3. Characteristic curves of storage modulus and loss factor towards temperature of Nafion 115 (a), casted BC and BC/Nafion (1:1) membranes before (b) and after annealing (c).

temperature over 80 °C. In other words, the Young's modulus of Nafion 115 was up to 220 MPa and the mechanical strength weakened at high temperature. Meanwhile, a peak was observed on the curve of loss factor, which demonstrates the glass transition point of Nafion at 123 °C. This result is in coincidence with that glass transition point of 125 °C reported by Chiou and Paul [47].

The plot of storage moduli of casted BC, pristine and annealed B1N1 membranes as function of temperature was displayed in Fig. 3b. The storage modulus of casted BC decreased when below the ice point, but increased dramatically as temperature transcended the ice point then followed by second descending at higher temperature over 50 °C. This might be attributed to the transition of states of water. As the temperature ascending from −50 °C to 0 °C, the ice inside membranes began melting, leading to the decrease of the mechanical strength. After that the melted liquid water had strong hydrogen bonds with the cellulose, which strongly enhanced the Young's modulus. However, high temperature forced water to evaporate gradually, leading to the reduction of hydrogen bonds and weakening the elastic modulus. No matter how much the storage modulus dropped, it was still up to 3000 MPa at least, in other words the Young's modulus of the casted BC membrane was 3 GPa at least, which was even stronger than that of the pristine dry BC membrane (1700 MPa) reported previously [31]. After blending with Nafion, the storage modulus of both pristine and annealed B1N1 membranes dropped to less than half of that of the casted BC. Despite that, they were still much stronger than that of Nafion 115, which demonstrates the blend membranes had good mechanical properties. It is noteworthy that the Young's modulus of annealed B1N1 membrane was slightly higher than that of pristine one, especially at the temperature lower than 0 °C, which indicates that annealing process enhanced the mechanical strength of B1N1.

Similar to the minimal value of storage modulus around zero point, Fig. 3c illustrates a peak of the loss factor of casted BC membrane at 8.7 °C. Generally, the temperature at the maximum value in tan δ corresponds to the glass–rubber transition. Wu et al. reported that glass transition temperature of cellulose was at 190 °C [48]. Therefore, 8.7 °C should not be the glass transition point of cellulose here but possibly the phase transition of water adsorbed on or combined with the cellulose. This peak was characteristic for BC. For blend membranes, two peaks were observed. For instance, on the curves of both pristine and annealed B1N1 membranes, one peak was around the ice point and the other one was around 145 °C, which represents the phase transition of BC and Nafion, respectively. The glass transition of Nafion in B1N1 was higher than that of Nafion 115 (123 °C), which might be attributed to the potential cross-linking or dehydration reaction between cellulose and Nafion after being heated over 100 °C. In brief, the DMA profiles revealed that Nafion in BC/Nafion blend membranes reserved its own properties and the annealing process enhanced the mechanical properties of membrane instead of negative influences.

3.4. Morphology of cross sections of BC/Nafion membranes

The cross-section features of the B1N1 and B1N7 membranes before and after annealing as well as the casted BC were investigated by using SEM and displayed in Fig. 4. As shown in Fig. 4A, the casted BC membrane demonstrated a typical laminated structure that should be attributed to the deposit of bunch of cellulose fibers and subsequent formation of hydrogen bonds interactions between fibers during drying.

After blending with the same amount of Nafion, the laminated structure of cellulose in B1N1 became denser while the interspaces between layers turned less obvious (Fig. 4B). The characteristic network structure of native BC disappeared and sheets-like BC was embedded with Nafion, illustrating a reinforced concrete-like structure. No significant difference was observed between pristine (Fig. 4B) and annealed (Fig. 4C) B1N1 membranes. But compared to the pristine B1N1, more tightness among the sheets after annealing might be arose from the reactions between cellulose fibers and Nafion as implied by the results of ATR-FTIR (Fig. 1), or from the glass–rubber transition under the heating circumstance as demonstrated by the results of DMA (Fig. 3), or from both of them.

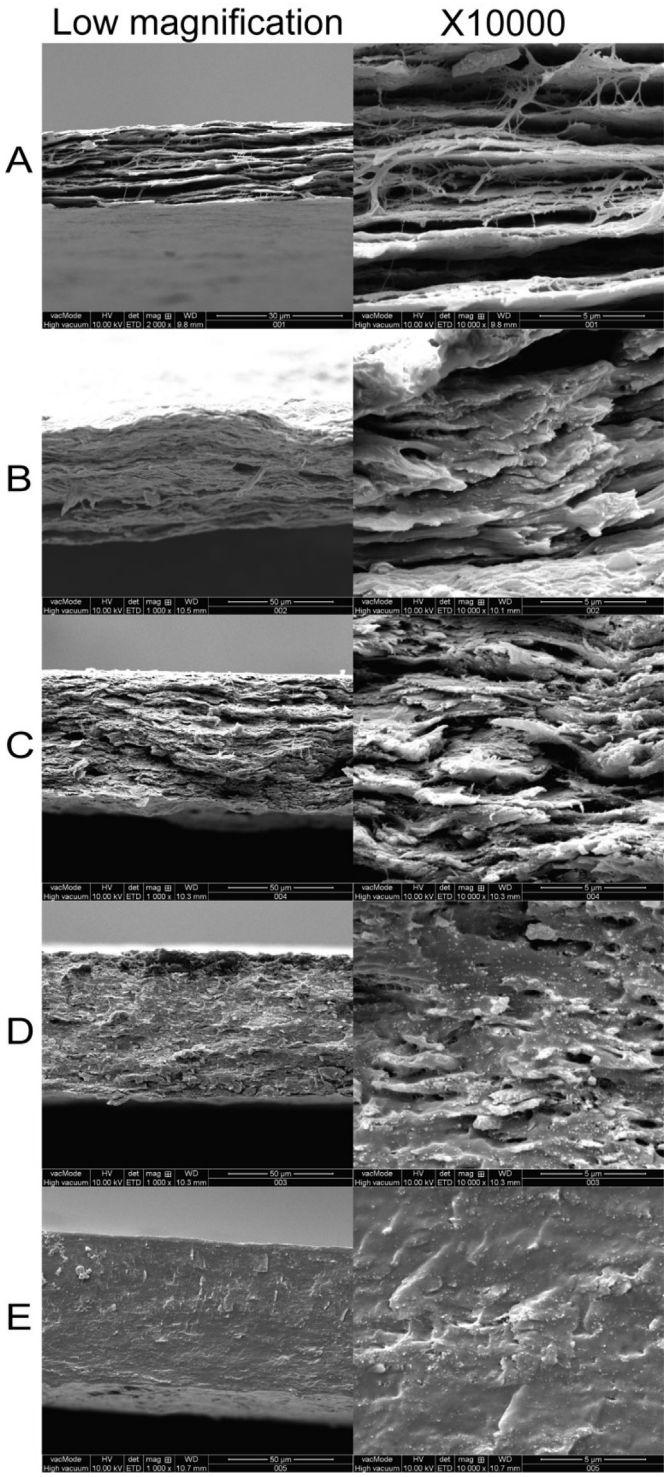

Fig. 4. SEM pictures of cross-sections of casted BC (A) and BC/Nafion membranes with different ratios of BC to Nafion, 1:1 (B, C) and 1:7 (D, E) before (B, D) and after (C, E) annealing at 1000× and 10000× magnification.

With the proportion of Nafion increasing, the cross-section of blend membrane such as B1N7 became much more condensed and less laminated (Fig. 4D). In spite of the disappearance of the obvious laminated structure, the cellulose fiber bunches were still embedded with Nafion. After being annealed, B1N7 displayed a different structure (Fig. 4E). The cross-sectional structure was not only compact but also uniform. The sheets-like structure was barely found in the SEM pictures (Fig. 4E). The reasons for the structure change might be the same as the annealed B1N1. Whereas, in view of the large percentage of Nafion in the blend membrane and lower T_g as tested by DMA, it could be reasonably assumed that the glass–rubber transition of Nafion dominated the structural change during annealing by dispersing and embedding cellulose fibers as well as flowing into and stuffing the pores or gaps in the membranes. In general, the annealing process was helpful to tighten the structure of membranes.

3.5. Water uptake and dimensional stability

The water uptake (WU) of the Nafion/BC blend membranes with different ratios of BC to Nafion before and after annealing are displayed in Fig. 5. Prior to annealing process, the pristine BC/Nafion blends demonstrated the water uptake of 0.9–1.2 g g^{-1}, which was slightly lower than that of casted BC (blue dotted line) but was far higher than that of Nafion 115 (red solid line) (in web version). The WU of samples increased with the proportion of Nafion added except B1N5. However, the WU dropped sharply to 0.2–0.3 g g^{-1} after annealing process. Furthermore, the WU decreased when more Nafion was incorporated, even lower than that of Nafion 115. The dramatic change might imply structural changes. As low water uptake is a desirable property for proton exchange membrane, the blends containing more Nafion should be more suitable for DMFC.

The dimensional properties were investigated by ASR and VSR. As shown in Fig. 6a, all the blend membranes enlarged less than 10% in area no matter whether they were annealed or not. The area swelling ratio was much lower than that of Nafion 115 (21%) marked with a red line (in web version). In general, the ASR increased with the rise of ratio of Nafion. However, Fig. 6b demonstrates that the VSR of BC/Nafion blends transited from high swelling ratios before annealing to a lower level than that of Nafion 115 (red line) (in web version) after annealing. Combining with the evaluation of ASR and VSR, it is obvious that the pristine blend membranes mainly swelled in thickness but the heating process eliminated the negative influences. Like the low water uptake, the enhancement of dimensional stability should be a desirable property for proton exchange membranes as well.

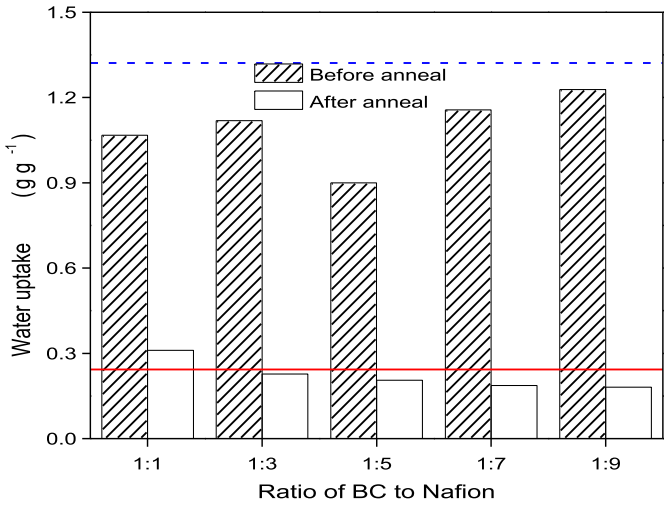

Fig. 5. Water uptake of BC/Nafion membranes before and after annealing. Blue dotted line: casted BC, Red solid line: Nafion 115. (For interpretation of the references to colour in this figure legend, the reader is referred to the web version of this article.)

3.6. Proton conductivity, methanol permeability and selectivity

Fig. 7 shows the proton conductivity of both pristine and annealed BC/Nafion membranes as a function of the ratio of BC to Nafion. In general, the more Nafion was incorporated with BC, the higher proton conductivity was obtained no matter whether the blend membranes were annealed or not. For example, the conductivities of pristine and annealed B1N1 were 0.015 and 0.008 S cm^{-1}, respectively, while those of B1N9 were 0.069 and 0.056 S cm^{-1}, respectively. Among all, the B1N9 exhibited the highest ion conductivity. The increase of conductivity could be ascribed to the introduction of charge carriers in Nafion. However, the conductivities lessened markedly after annealing. Considering the dramatic decrease of water uptake of annealed membranes (Fig. 5), the low mobility of proton under this circumstance might contribute to the phenomenon. In addition, the interactions

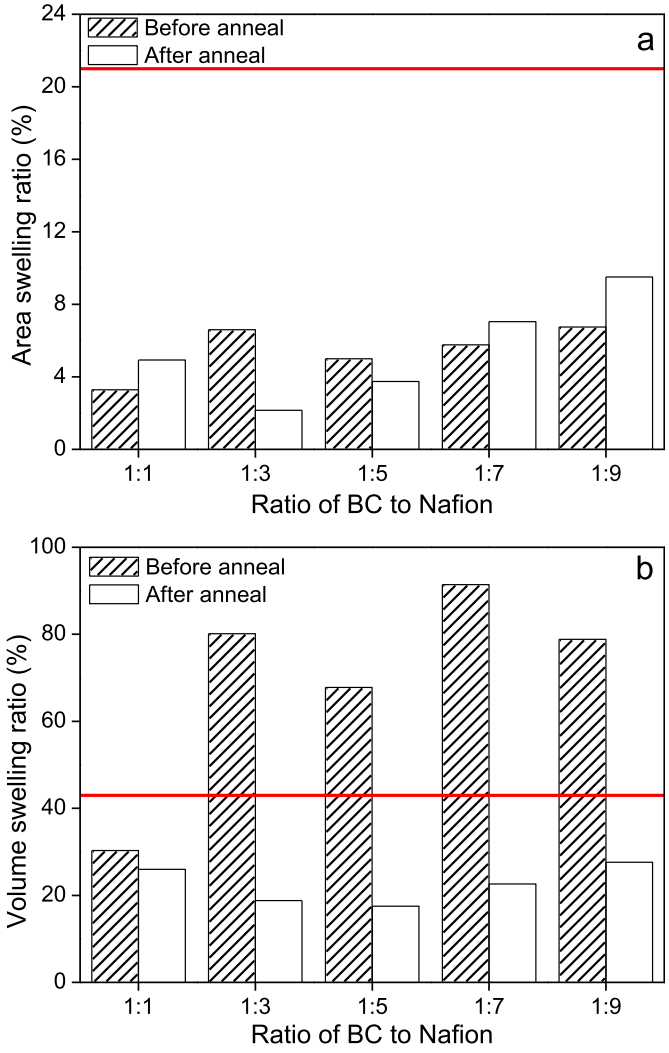

Fig. 6. Dimensional stability of BC/Nafion membranes before and after annealing including (a) area swelling ratio and (b) volume swelling ratio. Red lines represent the swelling ratios of Nafion 115. (For interpretation of the references to colour in this figure legend, the reader is referred to the web version of this article.)

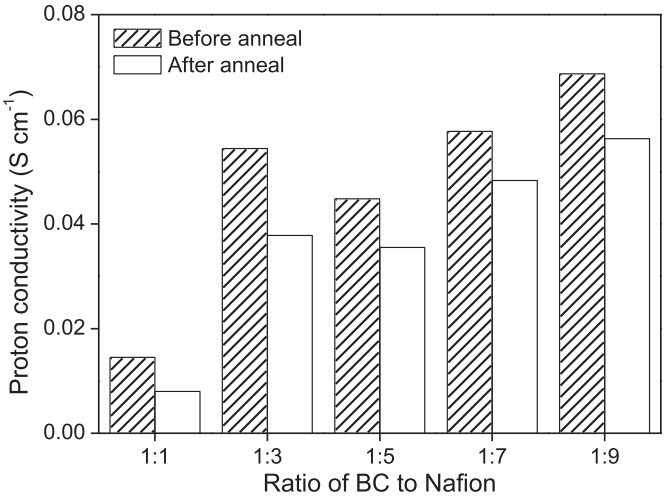

Fig. 7. Proton conductivity of BC/Nafion membranes before and after annealing.

between BC and Nafion during annealing might lead to the same result as well.

Methanol permeability of BC/Nafion blend membranes was investigated before and after annealing and the results are displayed in Fig. 8. Similarly, the methanol permeability of pristine blend membranes increased with the raised proportion of Nafion in the membranes. However, high methanol permeability is not a desirable property for proton exchange membranes, but a hindrance to the application in DMFC. As shown in Fig. 8, except B1N1 containing the most amount of BC, every pristine blend membrane displayed higher methanol permeability than Nafion 115 (red line) (in web version), which might be due to more Nafion proportion in the membranes. Fortunately, after annealed all blend membranes allowed much less methanol permeation, which should be attributed to the structural changes of membranes as observed by SEM (Fig. 4). Specifically, the methanol permeability of both annealed B1N1 and B1N7 reduced to 7.43×10^{-7} and 1.33×10^{-6} cm^2 s^{-1} respectively, which is lower than the red line marked as that of Nafion 115 and indicates their potentials in DMFCs.

In order to comprehensively confirm the blend membranes potentials in DMFCs, the selectivity of membranes were evaluated

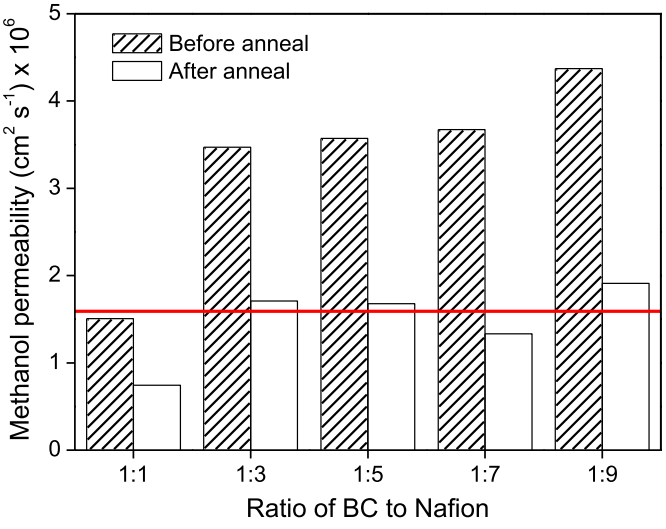

Fig. 8. Methanol permeability of BC/Nafion membranes before and after annealing. Red solid line: Nafion 115. (For interpretation of the references to colour in this figure legend, the reader is referred to the web version of this article.)

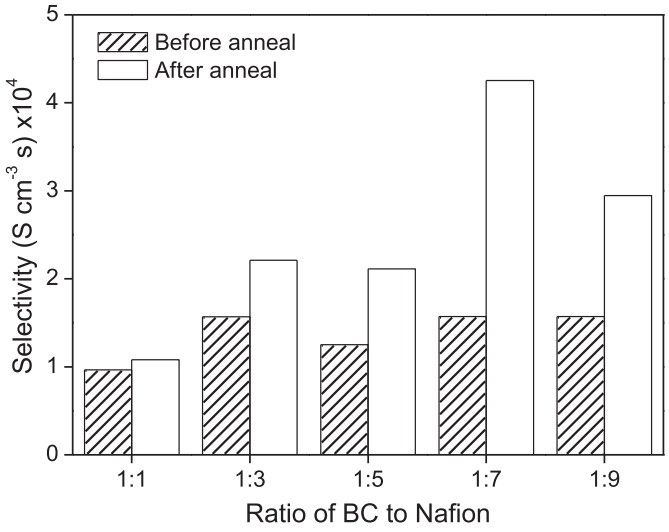

Fig. 9. The selectivity of BC/Nafion membranes before and after annealing.

and shown in Fig. 9. Since annealed membranes slightly decreased ion conductivity, (Fig. 7) but strongly declined methanol permeability (Fig. 8), their selectivity on proton was much more than that on methanol, compared to the pristine ones. As to pristine and annealed B1N1, both methanol permeability and proton conductivity were too low, which consequently diminished the selectivity to a great extent. Therefore, according to the logic in the literature [49,50], the most satisfactory candidate left for DMFCs was the annealed B1N7 with a selectivity of 4.26×10^4 S cm^{-3} s.

3.7. Single-cell performances

As chosen from the selectivity evaluation, both pristine and annealed B1N7 membranes were used to fabricate the membrane electrode assembly (MEA). In order to maximize the performance of DMFC, the MEAs were activated first in authentic H_2/O_2 single-cells prior to operation with 1 mol L^{-1} methanol aqueous solution as a fuel. The polarization curves and power density profiles of both PEMFC and DMFC were obtained and are displayed in Figs. 10 and 11, respectively. Fig. 10 shows that the open-circuit voltages (OCV) of both the pristine and annealed B1N7 reached around 0.91 V, which suggests a high activity of catalyst has been loaded on

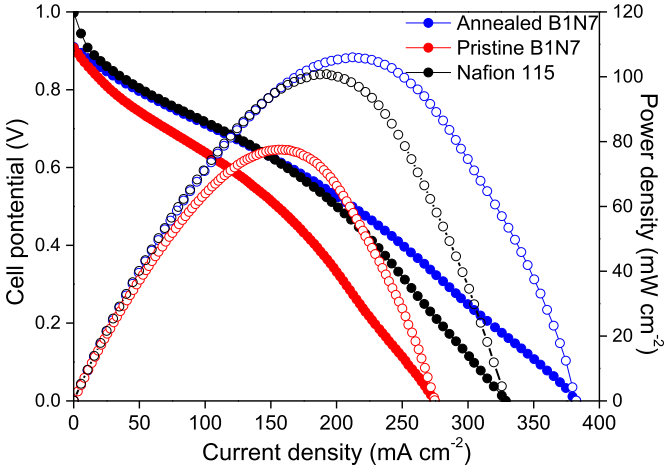

Fig. 10. PEMFC performances of pristine and annealed BC/Nafion (1:7) membranes as well as Nafion 115 at room temperature.

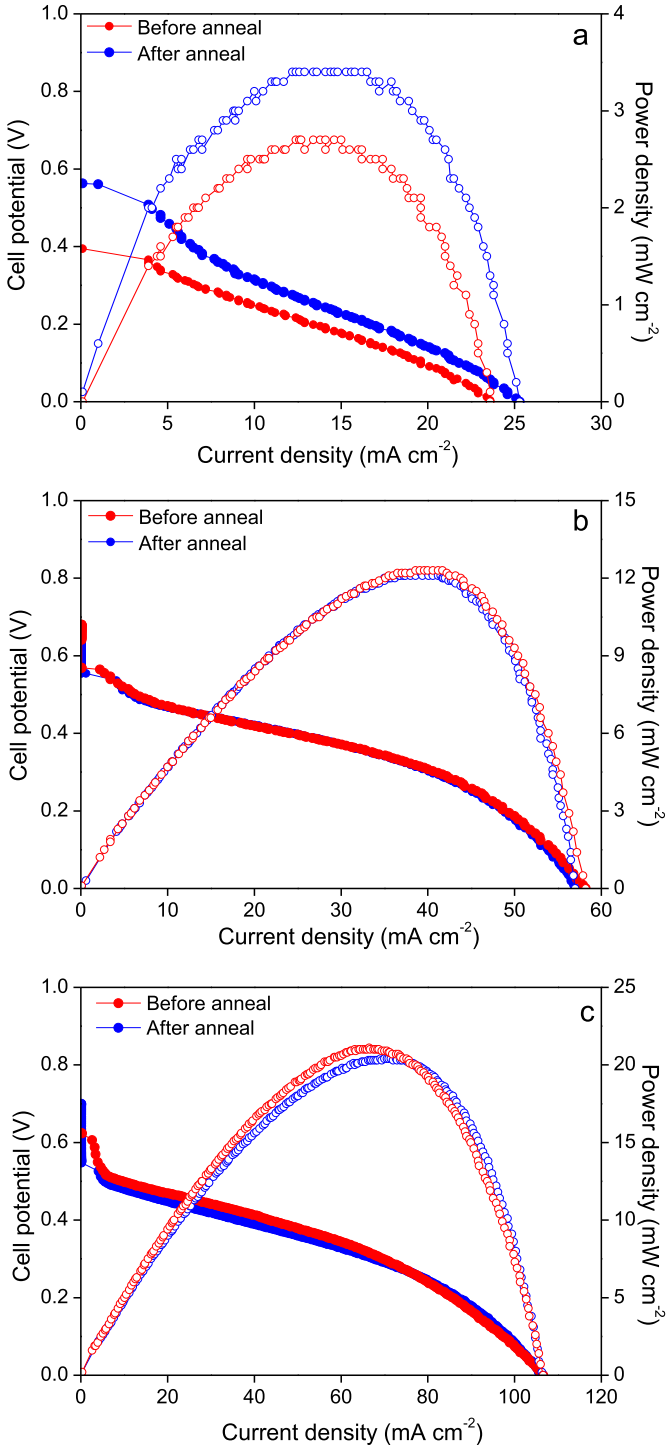

Fig. 11. DMFC performances of pristine and annealed BC/Nafion (1:7) membranes obtained at room temperature (a), 60 °C (b) and 80 °C (c).

carbon papers. However, the polarization curves showed differences with the elevation of current density. The MEA fabricated with an annealed B1N7 membrane demonstrated lower activation and ohmic overpotentials, resulted in maximum power density of 106 mW cm^{-2} and endurable current density of 382.4 mA cm^{-2} under an ambient temperature. Hence, it implies that the annealing process facilitated the performance of B1N7 in PEMFC. Slightly worse performance of Nafion 115 obtained at the same MEA fabrication and testing condition (black lines in Fig. 10, only giving a power density of 100.8 mW cm^{-2} and a maximum endurable current density of 328.7 mA cm^{-2}) makes the performance of B1N7 more trustworthy and reasonable.

After being fed with methanol as fuel, the MEAs equipped with either pristine or annealed B1N7 demonstrated their characteristic polarization curves and power density profiles obtained at room temperature, 60 °C and 80 °C, respectively (Fig. 11). Although the OCV of the annealed B1N7 was low at room temperature, it still reached about 0.6 V, which was higher than that of the pristine B1N7 (Fig. 11a). This result implies that less methanol crossover occurred through the membrane after annealing and is one of the benefits brought from the annealing process. Other merits as compared to the pristine B1N7, such as higher power density (3.2 mW cm^{-2}) and current density (23.8 mA cm^{-2}), were observed after annealing and are demonstrated in Fig. 11a. As the operating temperature rose to 60 °C, the performances of both pristine and annealed B1N7 were facilitated (Fig. 11b). All the parameters including the OCV, maximum power density and maximum current density of pristine and annealed B1N7 arose remarkably to 0.68 V, 12.3 mW cm^{-2}, and 58.2 mA cm^{-2}, as well as to 0.65 V, 12.2 mW cm^{-2}, and 57 mA cm^{-2}, respectively. Those aforementioned parameters as well as the overlapping of samples' polarization curves and power density profiles in Fig. 11b denote the slight differences from samples. When testing at 80 °C, OCV of the annealed B1N7 rose to 0.70 V while that of the pristine B1N7 dropped to 0.62 V (Fig. 11c). The elevation of operating temperature not only improved the activity of catalysts, resulting in the increase of OCV, but also drove more methanol molecules permeating through the membranes and oxidizing on the surface of Pt catalyst on cathode, leading to the decrease of OCV. Therefore, there was a balance between these two effects. Considering the methanol permeability of the pristine B1N7 shown in Fig. 8, it is reasonable to assume that high methanol crossover at 80 °C lowered the OCV of the pristine B1N7 but the enhancement of catalytic activity at high temperature dominated the main effect on OCV of annealed B1N7. Meanwhile, the peak power densities of pristine and annealed B1N7 were achieved at 21.1 and 20.4 mW cm^{-2} respectively (Fig. 11c). The similar performance and overlapping curves in Fig. 11b and c imply that the annealing process could not enhance the performance of B1N7 at higher temperature circumstance.

4. Conclusion

A series of novel proton exchange membranes have been prepared by blending bacterial cellulose pulp with Nafion solution for applications in both PEMFC and DMFC but also increased water uptake, Young's modulus, thermal and area swelling stabilities due to the characteristics of bacterial cellulose. Moreover, they developed some new features including the reinforced concrete structure and interactions of Nafion with cellulose. Annealing process made a positive effect on the properties of BC/Nafion membranes, including the dramatic decrease of water uptake, volume swelling ratio and methanol permeability as well as the increase of dense structure, Young's modulus and selectivity. The annealing could enhance the performance of the membranes in both PEMFC and DMFC under room temperature obviously. For annealed B1N7, the maximum power densities obtained in PEMFC and DMFC were 106 mW cm^{-2} and 20.4 mW cm^{-2}, respectively, which are much higher than those of BC-based membranes reported in the literature [28]. Overall, these preliminary results demonstrate that BC/Nafion blend membranes are promising candidates for both PEMFC and DMFC, and the annealing is a critical process during the fabrication.

Acknowledgments

This investigation was funded by Program for New Century Excellent Talents in University (NCET-12-0828), by the National Natural Science Foundation of China (51373031), the Science and Technology Commission of Shanghai Municipality (11230700600 and 12nm0500600), Opening Foundation of Zhejiang Provincial Top Key Discipline (20110927), the State Key Laboratory for Modification of Chemical Fibers and Polymer Materials (Donghua University) (13M1060106), the Fundamental Research Funds for the Central Universities (14D110502), and the China Scholarship Council. All the financial supports are gratefully acknowledged.

References

[1] J.H. Wee, J. Power Sources 173 (2007) 424–436.
[2] V. Neburchilov, J. Martin, H.J. Wang, J.J. Zhang, J. Power Sources 169 (2007) 221–238.
[3] M. Ahmed, I. Dincer, Int. J. Energy Res. 35 (2011) 1213–1228.
[4] J.H. Chen, D.R. Li, H. Koshikawa, M. Asano, Y. Maekawa, J. Memb. Sci. 362 (2010) 488–494.
[5] J. Qiao, S. Ikesaka, M. Saito, J. Kuwano, T. Okada, Electrochem. Commun. 9 (2007) 1945–1950.
[6] J.H. Kim, S.K. Kim, K. Nam, D.W. Kim, J. Memb. Sci. 415 (2012) 696–701.
[7] Y. Heo, S. Yun, H. Im, J. Kim, J. Appl. Polym. Sci. 126 (2012) E467–E477.
[8] C.Y. Tseng, Y.S. Ye, M.Y. Cheng, K.Y. Kao, W.C. Shen, J. Rick, J.C. Chen, B.J. Hwang, Adv. Energy Mater. 1 (2011) 1220–1224.
[9] Q. Zhao, Q.F. An, Y. Ji, J. Qian, C. Gao, J. Memb. Sci. 379 (2011) 19–45.
[10] C. Ling, D. Banerjee, W. Song, M.J. Zhang, M. Matsui, J. Mater. Chem. 22 (2012) 13517–13523.
[11] S. Mohanapriya, S. Bhat, A. Sahu, S. Pitchumani, P. Sridhar, A. Shukla, Energy Environ. Sci. 2 (2009) 1210–1216.
[12] N.W. DeLuca, Y.A. Elabd, J. Power Sources 163 (2006) 386–391.
[13] H.L. Lin, S.H. Wang, C.K. Chiu, T.L. Yu, L.C. Chen, C.C. Huang, T.H. Cheng, J.M. Lin, J. Memb. Sci. 365 (2010) 114–122.
[14] H.L. Lin, T.L. Yu, L.N. Huang, L.C. Chen, K.S. Shen, G.B. Jung, J. Power Sources 150 (2005) 11–19.
[15] H. Wu, Y.X. Wang, S.C. Wang, Acta Polym. Sin. (2002) 540–543.
[16] J.L. Qiao, T. Hamaya, T. Okada, Polymer 46 (2005) 10809–10816.
[17] J. Qiao, T. Hamaya, T. Okada, J. Mater. Chem. 15 (2005) 4414–4423.
[18] J. Hu, J. Luo, P. Wagner, C. Agert, O. Conrad, Fuel Cells 11 (2011) 756–763.
[19] T. Yang, C.T. Liu, Int. J. Hydrogen Energy 36 (2011) 5666–5674.
[20] E. Trovatti, L.S. Serafim, C.S.R. Freire, A.J.D. Silvestre, C.P. Neto, Carbohydr. Polym. 86 (2011) 1417–1420.
[21] M. Nogi, H. Yano, Adv. Mater. 20 (2008) 1849–1852.
[22] P. Gatenholm, D. Klemm, MRS Bull. 35 (2010) 208–213.
[23] D. Klemm, F. Kramer, S. Moritz, T. Lindstrom, M. Ankerfors, D. Gray, A. Dorris, Angew. Chem.-Int. Ed. 50 (2011) 5438–5466.
[24] V. Dubey, C. Saxena, L. Singh, K. Ramana, R. Chauhan, Sep. Purif. Technol. 27 (2002) 163–171.
[25] K. Ramana, K. Ganesan, L. Singh, World J. Microbiol. Biotechnol. 22 (2006) 547–552.
[26] Y. Kasai, A. Akahira, A. Abudula, K. Urayama, T. Takigawa, Kobunshi Ronbunshu 66 (2009) 130–135.
[27] A. Lam, D.P. Wilkinson, J.J. Zhang, Electrochem. Commun. 11 (2009) 1530–1534.
[28] C.W. Lin, S.S. Liang, S.W. Chen, J.T. Lai, J. Power Sources 232 (2013) 297–305.
[29] N.W. DeLuca, Y.A. Elabd, J. Memb. Sci. 282 (2006) 217–224.
[30] W. Helbert, H. Chanzy, T.L. Husum, M. Schülein, S. Ernst, Biomacromolecules 4 (2003) 481–487.
[31] G. Jiang, J. Qiao, F. Hong, Int. J. Hydrogen Energy 37 (2012) 9182–9192.
[32] J.L. Qiao, J. Fu, L.L. Liu, Y.Y. Liu, J.W. Sheng, Int. J. Hydrogen Energy 37 (2012) 4580–4589.
[33] L. Chaabane, G. Bulvestre, C. Larchet, V. Nikonenko, C. Deslouis, H. Takenouti, J. Memb. Sci. 323 (2008) 167–175.
[34] J.L. Qiao, T. Okada, H. Ono, Solid State Ionics 180 (2009) 1318–1323.
[35] Y.F. Huang, L.C. Chuang, A.M. Kannan, C.W. Lin, J. Power Sources 186 (2009) 22–28.
[36] C.W. Lin, R. Thangamuthu, C.J. Yang, J. Memb. Sci. 253 (2005) 23–31.
[37] B. Li, J.L. Qiao, D.J. Yang, R. Lin, H. Lv, H.J. Wang, J.X. Ma, Int. J. Hydrogen Energy 35 (2010) 5528–5538.
[38] S.Y. Oh, D.I. Yoo, Y. Shin, H.C. Kim, H.Y. Kim, Y.S. Chung, W.H. Park, J.H. Youk, Carbohydr. Res. 340 (2005) 2376–2391.
[39] S. Gea, C.T. Reynolds, N. Roohpour, B. Wirjosentono, N. Soykeabkaew, E. Bilotti, T. Peijs, Bioresour. Technol. 102 (2011) 9105–9110.
[40] L. Chen, F. Hong, X. Yang, S. Han, Bioresour. Technol. 135 (2013) 464–468.
[41] S.A. Perusich, J. Appl. Polym. Sci. 120 (2011) 165–183.
[42] A.C. Fernandes, E.A. Ticianelli, J. Power Sources 193 (2009) 547–554.
[43] K. Hongsirikarn, X.H. Mo, J.G. Goodwin, S. Creager, J. Power Sources 196 (2011) 3060–3072.
[44] M. Roman, W.T. Winter, Biomacromolecules 5 (2004) 1671–1677.
[45] F. Hong, J. Biotechnol. 136 (Supplement) (2008) S433.
[46] S.D. Clas, K. Lalonde, K. Khougaz, C.R. Dalton, R. Bilbeisi, J. Pharm. Sci. 101 (2012) 558–565.
[47] J.S. Chiou, D.R. Paul, Industrial Eng. Chem. Res. 27 (1988) 2161–2164.
[48] Y.B. Wu, S.H. Yu, F.L. Mi, C.W. Wu, S.S. Shyu, C.K. Peng, A.C. Chao, Carbohydr. Polym. 57 (2004) 435–440.
[49] M.M. Hasani-Sadrabadi, E. Dashtimoghadam, F.S. Majedi, K. Kabiri, N. Mokarram, M. Solati-Hashjin, H. Moaddel, Chem. Commun. 46 (2010) 6500–6502.
[50] H.C. Chien, L.D. Tsai, C.P. Huang, C.Y. Kang, J.N. Lin, F.C. Chang, Int. J. Hydrogen Energy 38 (2013) 13792–13801.